

## Local Textures and Grain Boundaries In Voided Copper Interconnects\*

R.R. KELLER<sup>1</sup>, J.A. NUCCI<sup>2</sup>, and D.P. FIELD<sup>3</sup>

<sup>1</sup>National Institute of Standards and Technology, Materials Reliability Division, 325 Broadway, Boulder, CO 80303;

<sup>2</sup>Cornell University, School of Electrical Engineering, Phillips Hall, Ithaca, NY 14853;

<sup>3</sup>TexSEM Laboratories, Inc., 226 West 2230 North #120, Provo, UT 84604

### Abstract

We have characterized grain boundary structures and local textures in stress voided copper lines. Grain boundary misorientations as well as the tilt and twist character of boundaries were measured using electron backscatter diffraction in the scanning electron microscope in conjunction with focussed ion beam images. We have summarized data for a number of boundaries immediately adjacent to voids and made comparisons to boundaries from regions that remained intact. These data were acquired from the same lines, and so represent measurements from material with identical histories. Significant local variations in microstructure were observed. Local (111) textures of grains near voids were of lower strength than those away from voids. Grain boundaries intersecting voids were of higher angle character with significant twist components. These results suggest that local regions associated with more favorable kinetics are more susceptible to void formation and growth.

\*Partial contribution of the U.S. Department of Commerce. Not subject to copyright in the U.S.

## INTRODUCTION

We present in this paper the results of a study on effects of local variations in the microstructure of oxide-passivated copper interconnects on stress-induced voiding reliability. By "local," we refer to characteristics of microstructure on the scale of individual grains and grain boundaries. Such an approach to understanding interconnect reliability is valuable since manufacturing trends include scaling of interconnect structures well into the sub-micrometer regime<sup>1,2</sup> leading to lines with thicknesses and widths of the order of one or two grain diameters. As line dimensions continue to decrease, we intuitively expect local variations in thin film microstructure to play an increasingly important role in controlling integrated circuit device reliability. Further, local characterizations provide valuable insight into the effects of alternative processing schemes such as the damascene approach<sup>3</sup>.

The effects of grain size<sup>4</sup> and average texture<sup>5,6</sup> have been investigated for aluminum and aluminum alloy lines subjected to stress voiding conditions. Larger-grained materials were found to have better resistance to void formation and growth, while lines showing stronger average texture also showed better resistance to voiding. An interesting, apparent contradiction to the influence of average texture on stress voiding in aluminum has also been reported<sup>7</sup>, with increased voiding in lines of stronger average texture. Clearly, further investigations of stress voiding in aluminum should be conducted. Considerably less information about microstructural influences is available for copper films, since the first observation of stress voiding in copper was made only in 1992.<sup>8</sup> Although some investigations have addressed average strain measurements and stress relaxation in copper<sup>9,10</sup>, they did not include stress voiding effects, since only blanket films were treated. Stress voiding in passivated 2  $\mu\text{m}$ -wide copper lines was studied using X-ray diffraction strain measurements and *in-situ* high voltage scanning electron microscopy (SEM) observations of voids<sup>11</sup>. That work showed that thermal stress-induced voiding in copper can be significant. However, due to the *in-situ* testing approach,

microstructural features beyond void geometries were not observable through the passivation layer. The effect of linewidth on stress voiding in copper was observed<sup>12</sup> and explained by noting that for a constant grain size, narrow lines have fewer triple junctions than wide lines. This reduced the number of potential nucleation sites in narrow lines, and indeed resulted in less void formation. Another study on copper reliability suggested similar effects<sup>13</sup>. Further recent work on copper<sup>14, 15, 16</sup> showed that copper lines with stronger average (111) texture exhibited better stress voiding reliability, a result similar to that found for aluminum lines. That work also showed that there can be significant variations in local texture within a line. Those regions showing void formation were correlated with locally weaker texture.

An interesting similarity among several of the investigations described above<sup>3,5-7,14-16</sup> is that the researchers used the electron backscatter diffraction (EBSD) technique to gain information from the lines. This seems to be a technique ideally suited for investigating the microstructures of fine lines, since sampling volumes are of approximate diameter 0.1 to 0.5  $\mu\text{m}$ , roughly the scale of the grain size. Of the studies mentioned above, only the work of Rodbell and co-workers<sup>7</sup> and Nucci and co-workers<sup>14-16</sup> has so far taken advantage of this spatial resolution in terms of characterizing the effects of local variations in microstructure on stress voiding. We present in this paper more details of the work described in references 14 and 15, addressing local microstructure and grain boundary effects on stress voiding in copper lines.

## EXPERIMENTAL

Copper lines of width 0.75 to 2.0  $\mu\text{m}$  and thickness 0.5  $\mu\text{m}$  were fabricated using electron-beam evaporation and a trilayer lift-off stack, with processing details provided elsewhere<sup>12</sup>. A 50 nm layer of tantalum was used as both a diffusion barrier and adhesion layer between the copper and surrounding silicon dioxide. The lift-off stack ensured that the lines had

vertical sidewalls. The lines were passivated with 1.2  $\mu\text{m}$  of plasma-enhanced chemical vapor deposited  $\text{SiO}_2$ .

Some samples were annealed for 1 h at 450°C prior to passivation deposition in order to strengthen texture, since this was known to improve overall stress voiding reliability in aluminum-based lines<sup>5,6</sup>. Others were not subjected to the pre-passivation anneal. All samples were subjected to an annealing treatment of 1h at 400°C after passivation, to induce thermal stresses. All anneals were run in vacuum at a base pressure of  $1 \times 10^{-5}$  Pa ( $2 \times 10^{-7}$  torr). The final anneal concluded with furnace cooling to room temperature. Passivation and overlying tantalum layers were removed by reactive ion etching in a  $\text{CF}_4$  ambient to expose the copper surfaces for EBSD and focussed ion beam (FIB) analyses. An earlier paper<sup>12</sup> described void statistics for these samples and distinguished between samples that were pre-passivation annealed and those that were not. It was confirmed there that the samples that underwent the pre-passivation anneal exhibited superior voiding reliability, while maintaining an equivalent grain size. In this paper, we do not distinguish between annealing treatments, but rather solely between voided and unvoided regions.

Figure 1 shows a scanning electron microscope (SEM) and FIB image of the same void within one of the lines. The grain structure is clear in the FIB image, due to ion channeling contrast. FIB imaging and subsequent image analysis indicated that the samples had a monomodal grain size distribution, with an average grain diameter of 0.56  $\mu\text{m}$ , as measured after the post-passivation anneal. The uncertainty is approximately 0.03  $\mu\text{m}$  in measuring approximately 100 grains from the FIB images.

EBSD patterns were collected from two types of positions within each line. Figure 2 shows the diffraction data collection scheme. The electron beam was positioned first at locations immediately adjacent to voids. 4 to 8 diffraction patterns were collected within approximately

0.3  $\mu\text{m}$  of the edges around each of 19 voids. Orientations determined from these patterns were grouped together and comprise the data from voided regions. Patterns from arrays of beam positions in unvoided regions of the lines were collected for comparison. The unvoided data sampled several micrometers along the line length and the entire line width for 1 and 2  $\mu\text{m}$  wide lines. 94 diffraction patterns adjacent to voids and 132 diffraction patterns within unvoided regions were analyzed.

## RESULTS

The EBSD data were first evaluated in terms of average textures. Figure 3 shows the (111) pole figure for the samples, independent of electron beam location. (111) texture strength was quantified by calculating an orientation distribution function and then recalculating the (111) distribution as a function of tilt angle away from the sample normal. Such a pole plot distribution<sup>14,15</sup> revealed a central ( $0^\circ$  from sample normal) orientation density of approximately 7.2 times random.

Differences in *local* texture strength within the samples were determined next. Figure 4(a) shows a (111) pole figure for grains immediately adjacent to voids. Figure 4(b) shows a (111) pole figure for grains in unvoided regions of the same lines. Comparison of the data in these two figures revealed that local textures in voided regions were weaker than textures in intact regions. Pole plot distributions revealed that the texture associated with voided regions is approximately 20 to 25 % weaker than that in regions that remained intact.

Next, grain boundary misorientation angles were quantitatively analyzed. Although a misorientation angle provides an incomplete structural description of a grain boundary, it can be correlated to physical properties such as diffusivity. Grain boundary misorientation angles were determined by following the procedure described by Warrington and Bufalini<sup>17</sup>. Angles were

determined for all adjacent pairs of patterns. Misorientation angles of less than  $2^\circ$  were treated as originating from a pair of patterns from a single grain, since such small rotations may occur due to surface deformation or dislocation structures. Once all misorientations were determined, the data were summarized into separate files for voided and unvoided beam locations. Figure 5 shows the boundary misorientation angle results. The angles from unvoided regions include a higher proportion of low angle boundaries than those from voided regions. If we define low angle as  $\leq 16^\circ$ , then the proportions are approximately 13% low angle for unvoided regions, and 5% low angle for boundaries intersecting voids. The effect is stronger yet for angles below  $8^\circ$ , where the proportions are 9% low angle for unvoided regions and 2% low angle for boundaries intersecting voids. The distributions for both voided and unvoided regions fall between those for a perfect (111) fiber texture and a randomly textured material<sup>18</sup>, as also expected from the pole figure analysis.

Misorientation angles were also used in conjunction with FIB images to determine the relative tilt and twist character of grain boundaries. In simple terms, a grain boundary is of pure tilt character when the misorientation axis lies parallel to the grain boundary plane. A material with perfect (111) fiber texture will have entirely pure tilt boundaries. A boundary is of pure twist character when the misorientation axis lies perpendicular to the boundary plane. We followed the procedure described by Randle<sup>19</sup>. The total misorientation is decomposed into tilt and twist components by first determining the two grain boundary plane normals, with reference to the crystal axes for each grain associated with a boundary<sup>20</sup>. The tilt angle component is the angle between the two boundary plane normals, while the twist component is a subsequent rotation about one of the boundary normals. One assumption made in this analysis is that all grain boundary planes were situated exactly normal to the film plane, in other words, we assumed perfect columnar growth. While not exactly correct, this assumption is reasonable, based on a series of through-thickness FIB images collected from one set of these lines. We estimate that the error introduced by this assumption is no more than a few degrees for the

average grain boundary. Due to a lack of sufficient FIB data, tilt and twist character determinations for unvoided regions were not made. However, their contributions were inferred from texture strengths. Figure 6 shows a plot of tilt angle versus twist angle for grains adjacent to voids. The line drawn at  $45^\circ$  from the origin indicates positions in this plot where boundaries are of exactly 50% tilt and 50% twist character. Points below the line are more twist-like, while points above the line are more tilt-like. The spread of the data indicates a fairly wide distribution in boundary structures, but no boundaries approached pure tilt character. The average boundary has a tilt component of  $24.6^\circ$  and a twist component of  $29.0^\circ$ . In other words, the average boundary intersecting a void is of slightly more twist than tilt character. This finding correlates back to a weaker local texture associated with grains immediately adjacent to voids.

## DISCUSSION

These results show that significant local variations in texture and grain boundary structure exist within narrow lines of copper. Grain boundary structures and hence properties should vary more for materials with a weaker texture<sup>21</sup> in comparison to those with a strong texture. We postulated<sup>14</sup> that for copper lines, one consequence of the locally weaker texture associated with grains adjacent to voids was the presence of a general mixture of tilt and twist structures for the boundaries intersecting voids. While it was already clear that a non-perfect (111) texture in combination with columnar grain growth would lead to some type of tilt/twist mixture, it was not obvious how much twist character would be present in those boundaries. The boundary plane and tilt/twist analysis has indeed revealed that grain boundaries intersecting voids exhibit a significant proportion of twist character. In fact, although the (111) texture for grains adjacent to voids was weaker than that for unvoided regions, it still showed a strength of approximately 6.3 times that expected for a random structure. The boundaries, though, exhibited more twist than tilt character on average. It appears that even relatively small deviations from perfect texture will lead to a large population of twist grain boundaries. Such boundaries

generally exhibit isotropic diffusivities in the boundary plane<sup>22</sup>, and thus represent potentially long pathways for relatively easy diffusion in directions parallel to the film surface. This boundary structure can accommodate the mass transport necessary for void growth. Stronger texture, with the associated higher population of tilt boundaries, suggests that diffusion is strongly preferred in the direction of the edge dislocations making up the boundary, namely from the film surface down to the film/substrate interface. Since the diffusion distance in the film plane is then very limited, this is not an efficient means for removing many atoms from a void nucleation site. The presence of groups of twist grain boundaries in some regions of the copper lines implies that those regions are susceptible to faster void growth even before a driving force for atom migration exists. Simply controlling overall texture strength is not sufficient for improving resistance to stress voiding; the local variations in grain orientations must also be considered. It is also likely that an individual grain oriented far from (111) will have little effect on void growth. Rather, groups of off-(111) grains result in the twist boundaries that lead to faster void growth.

The grain boundary misorientation angle analysis supports the above discussion further by indicating that boundaries intersecting voids are also generally of higher angle character. Neglecting coincidence relationships, diffusivity increases with increasing misorientation angle<sup>6,23</sup>. Such variations in diffusivity as a function of misorientation hold generally for lower angles, where "low angle" is conventionally defined as angles less than about 15°;<sup>24</sup> note that our analysis defined the high-low distinction at 16°. The exact number is a consequence of the dislocation arrangement making up the boundary and will vary somewhat for different materials. Below about 15°, the spacing of dislocations making up a boundary is sufficiently large that there is not a significant contribution from diffusion along their cores. Such a boundary would have an overall lower diffusivity than one containing more dislocations. Above 15°, the dislocations become very closely spaced and their core structures begin to overlap, thereby increasing overall boundary energy very little with further increases in angle. Diffusion then

becomes relatively easy in the plane of the boundary, neglecting further specifics such as tilt and twist structure. Perhaps a more appropriate description of the misorientation angle effect would be that grain boundaries intersecting voids exhibit an absence of low angle misorientations.

We speculate on the effects of specific combinations of the degree of tilt/twist character and the misorientation angle. We suggest that the most void-susceptible boundary would be one that was of strong tilt-B or twist character combined with a relatively large misorientation angle. Further, triple junctions composed of the intersection of two or three such boundaries might represent the most favorable structure for void growth, since there are efficient diffusion paths in many directions. This presents an interesting contrast to the case of electromigration in polycrystalline lines. In the presence of the unidirectional driving force provided by an electric current, electromigration void formation and growth occurs at sites of flux divergence. Stress voiding is different in that the driving force for diffusion away from a void is radial, due to the local relaxation of biaxial tensile stresses at the void. A cluster of three high diffusivity (tilt-B, twist and higher angle) boundaries intersecting in a triple junction, in the presence of such a radial stress gradient, provides an efficient means for locally relaxing the biaxial tensile stress state through void growth. However, for electromigration, such a cluster of boundaries should not lead to as severe a flux divergence as a cluster composed of low diffusivity boundaries at the upwind end and high diffusivity boundaries at the downwind end of a void. Whether such effects play a significant role remains to be seen.

## SUMMARY AND CONCLUSIONS

Measurements of local texture, grain boundary misorientation angle, and the tilt/twist character of grain boundaries revealed significant variations in the local microstructure of copper lines. Grains near voids exhibited lower texture strength than those in unvoided regions. Grain boundaries intersecting voids had a very small proportion of low angle boundaries, and showed

considerable twist character. We suggest that grain boundaries intersecting voids allowed for more diffusion than those boundaries within regions that remained intact. Local variations in microstructure may therefore play an important role in affecting interconnect reliability.

#### ACKNOWLEDGMENTS

This work was supported by Semiconductor Research Corporation Contract No. 96-IJ-426.001 and by the NIST Office of Microelectronic Programs. Samples were fabricated at the Cornell Nanofabrication Facility and analyzed at the Materials Science Center at Cornell University and TexSEM Laboratories, Inc.

## Figure Captions

1. SEM image (left) and FIB image (right) of the same void within a line.
2. Schematic illustration showing electron beam positions probed within SEM for EBSD pattern collection. Stars represent positions in regions that remained intact after cooling to room temperature. Circles represent positions in regions immediately adjacent to voids.
3. (111) pole figures showing overall average texture for the samples.
4. (111) pole figures showing local textures associated with: (a) voided regions; (b) unvoided regions.
5. Histogram showing distribution in grain boundary misorientation angles, separated according to voided and unvoided locations.
6. Plot of degree of grain boundary tilt and twist character for boundaries intersecting voids. Points in the lower right portion of the plot are more twist-like. No distinction between tilt-A and tilt-B boundaries was made (see text).

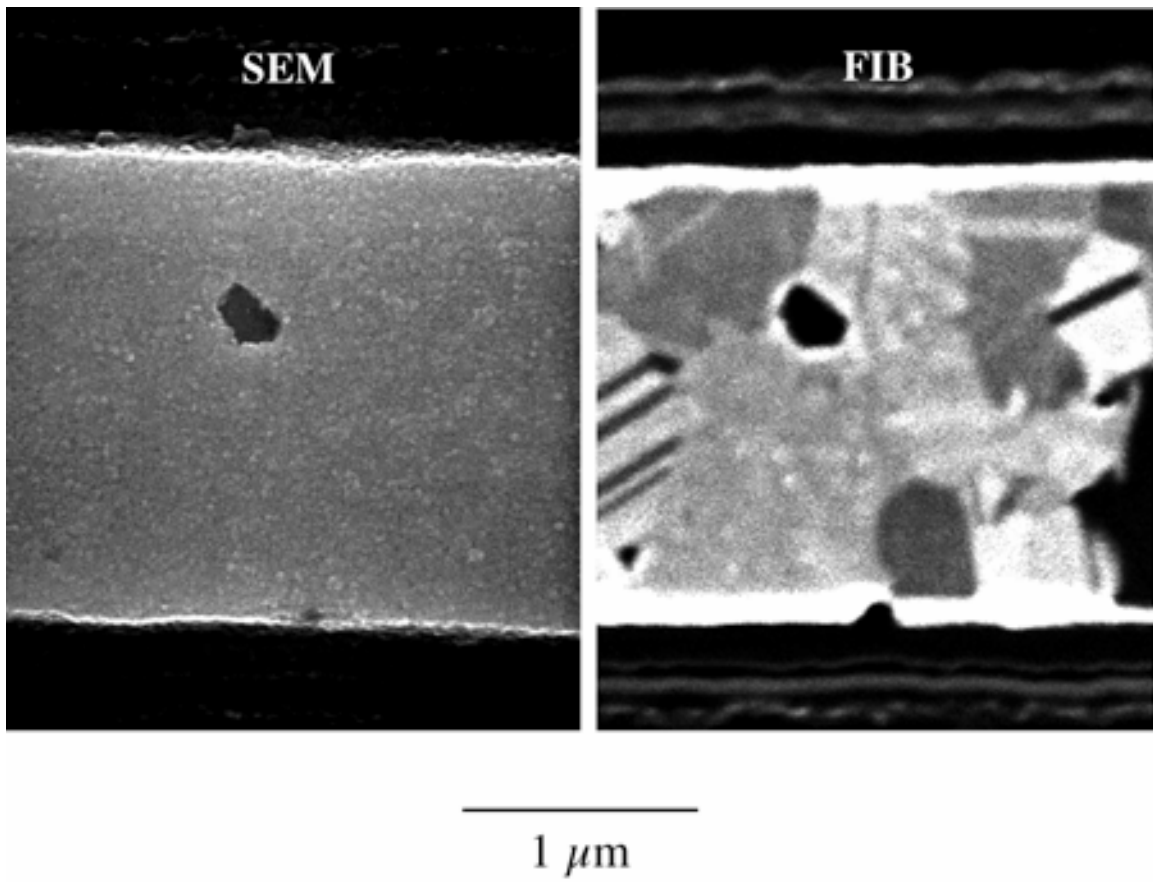


Figure 1

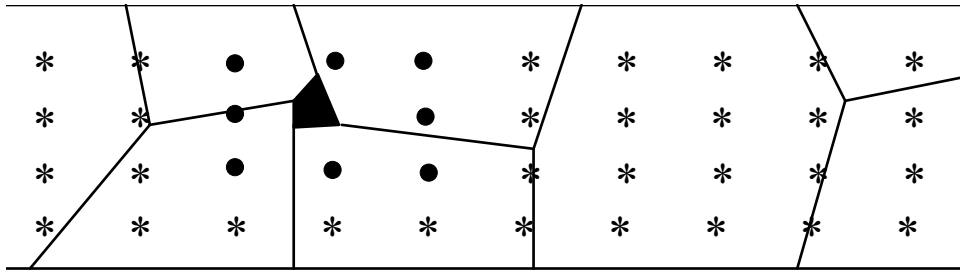


Figure 2

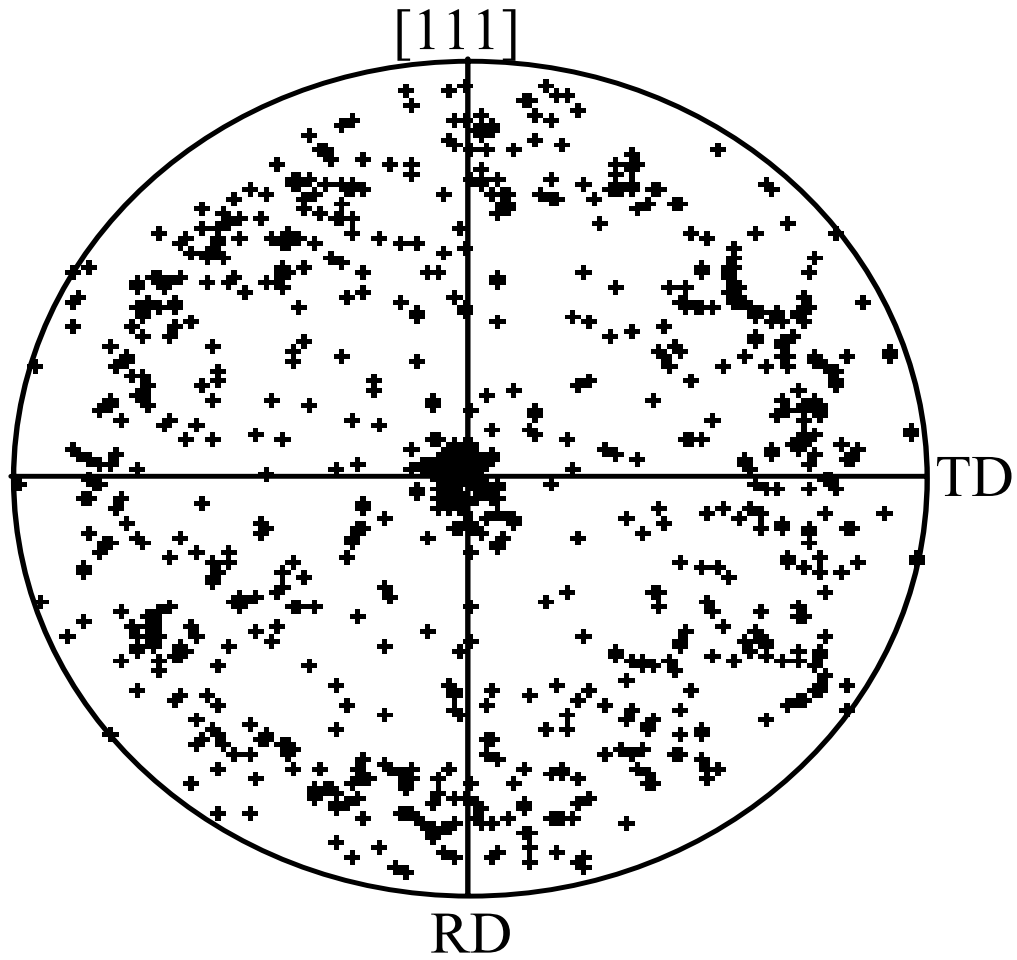
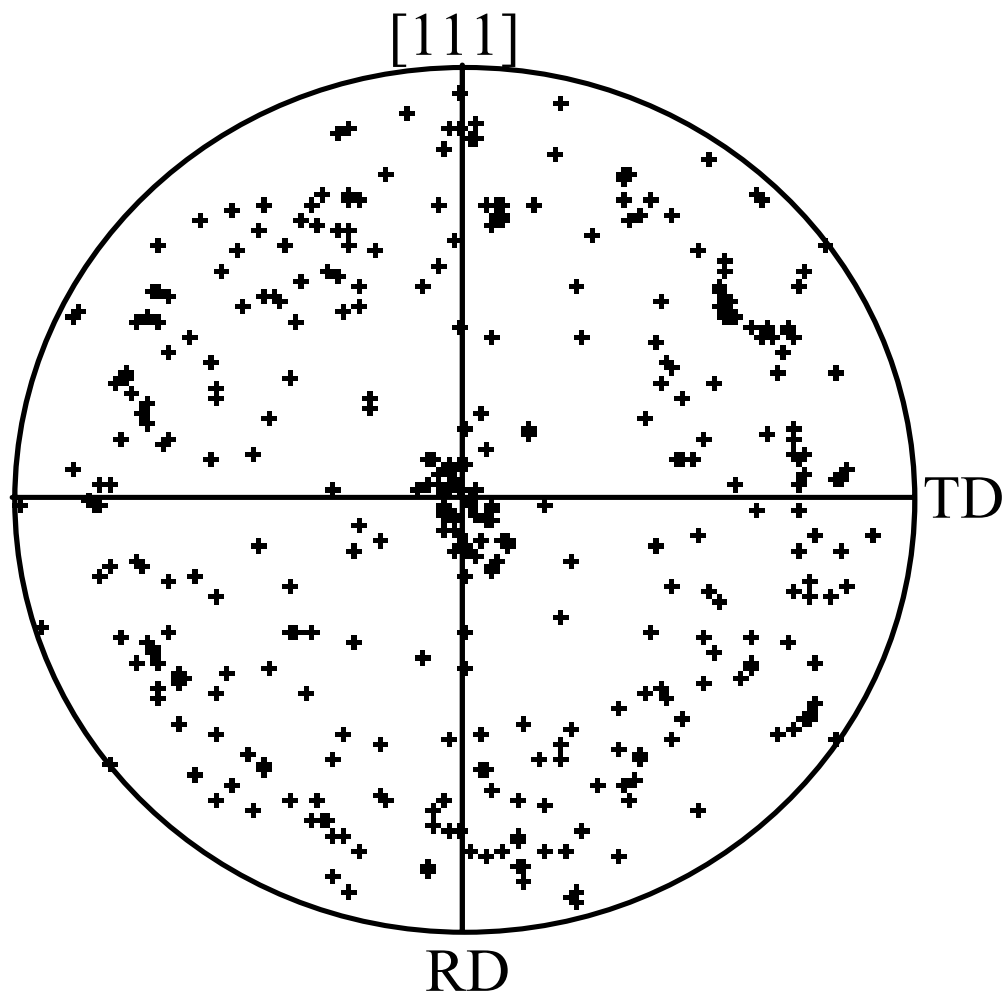
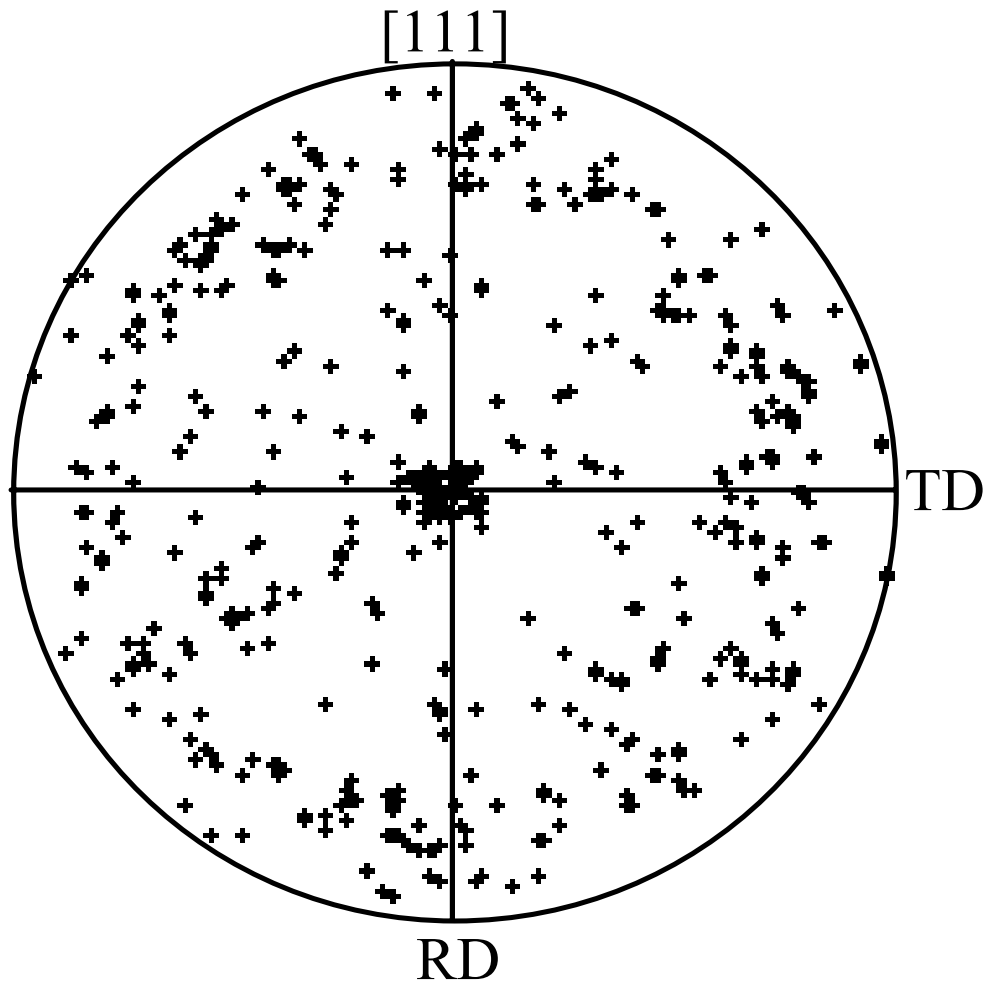


Figure 3



(a)



(b)

Figure 4

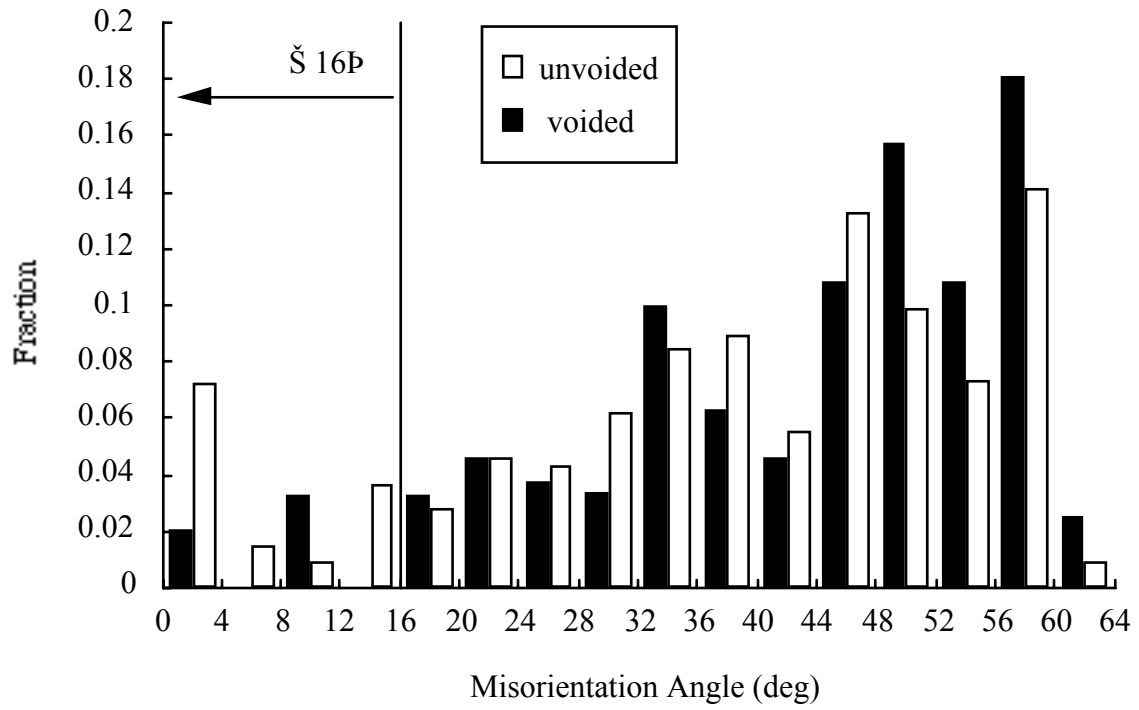


Figure 5

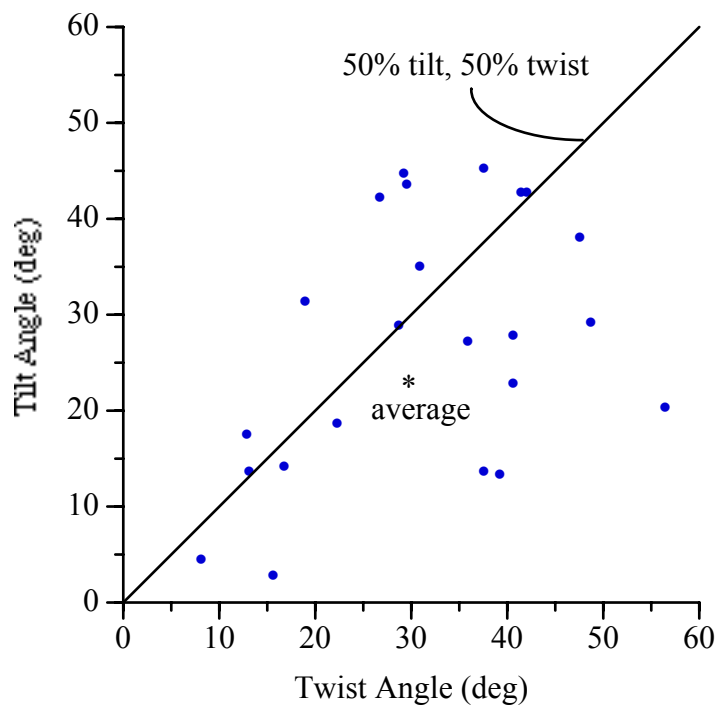


Figure 6

## REFERENCES

---

1. *The National Technology Roadmap for Semiconductors*, (San Jose, CA: Semiconductor Industry Association, 1994), p. 94.
2. M. Bohr, "Scaling of High Performance Interconnects," Proc. Advanced Metalization and Interconnect Systems for ULSI Applications in 1996 (Pittsburgh: MRS), in press.
3. J.E. Sanchez, Jr., P.R. Besser, and D. Field, "The Microstructure of Damascene Processed Al-Based Metallization Interconnects for Integrated Circuit Applications," Appl. Phys. Lett., submitted (1997).
4. J.T. Yue, W.P. Funsten, and R.V. Taylor, Proc. 23rd Int. Rel. Phys. Symp. (New York: IEEE, 1985), p. 126.
5. S. Kordic, R.A.M. Wolters, and K.Z. Troost, J. Appl. Phys. 74, 5391-5394 (1993).
6. S.C. Wardle, B.L. Adams, C.S. Nichols, and D.A. Smith, Mat. Res. Soc. Symp. Proc. Vol. 343, 665-670 (1994).
7. K.P. Rodbell, J.L. Hurd, and P.W. DeHaven, Mat. Res. Soc. Symp. Proc. Vol. 403, 617-626 (1996).
8. P. Børgesen, J.K. Lee, R. Gleixner, and C.-Y. Li, Appl. Phys. Lett. 60, 1706-1708 (1992).
9. E.M. Zielinski, Ph.D. Dissertation, Stanford University, (1995).
10. R.P. Vinci and J.C. Bravman, Mat. Res. Soc. Symp. Proc. Vol. 309, 269-273 (1993).
11. R.P. Vinci, T.N. Marieb, and J.C. Bravman, Mat. Res. Soc. Symp. Proc. Vol. 309, 229-234 (1993).
12. J.A. Nucci, Y. Shacham-Diamand, and J.E. Sanchez, Jr., Appl. Phys. Lett. 66, 3585-3587 (1995).
13. D.D. Brown, Ph.D. Dissertation, Cornell University (1996).
14. J.A. Nucci, R.R. Keller, J.E. Sanchez, Jr., and Y. Shacham-Diamand, Appl. Phys. Lett. 69, 4017-4019 (1996).

15. D.P. Field, J.A. Nucci, and R.R. Keller, Proc. 22nd Int. Symp. for Testing and Failure Analysis (Los Angeles: ASM International, 1996), p. 351-355.
16. J.A. Nucci, Ph.D. Dissertation, Cornell University (1996).
17. D.H. Warrington and P. Bufalini, Scripta Metall. 5, 771-776 (1971).
18. D.P. Field and D.J. Dingley, J. Elect. Mater. 25, 1767-1771 (1996).
19. V. Randle, The Measurement of Grain Boundary Geometry (Philadelphia: Institute of Physics, 1993), pp. 29-32.
20. *Ibid.*, pp. 106-111.
21. D.B. Knorr, D.P. Tracy, and K.P. Rodbell, Appl. Phys. Lett. 59, 3241-3243 (1991).
22. H. Gleiter and B. Chalmers, "Grain-Boundary Diffusion," Prog. Mat. Sci. 16, ed. B. Chalmers, J.W. Christian, and T.B. Massalski (New York: Pergamon Press, 1972) pp. 77-112.
23. D. Turnbull and R.E. Hoffman, Acta Metall. 2, 419 (1954).
24. W.T. Read and W. Shockley, Phys. Rev. 78, 275-289 (1950).